Picosecond superconducting single-photon optical detector

G. N. Gol'tsman,[a] O. Okunev, G. Chulkova, A. Lipatov, A. Semenov, K. Smirnov, B. Voronov, and A. Dzardanov
Department of Physics, Moscow State Pedagogical University, Moscow 119435, Russia

C. Williams and Roman Sobolewski[b]
Department of Electrical and Computer Engineering and Laboratory for Laser Energetics, University of Rochester, Rochester, New York 14627-0231

(Received 22 January 2001; accepted for publication 1 June 2001)

We experimentally demonstrate a supercurrent-assisted, hotspot-formation mechanism for ultrafast detection and counting of visible and infrared photons. A photon-induced hotspot leads to a temporary formation of a resistive barrier across the superconducting sensor strip and results in an easily measurable voltage pulse. Subsequent hotspot healing in ~30 ps time frame, restores the superconductivity (zero-voltage state), and the detector is ready to register another photon. Our device consists of an ultrathin, very narrow NbN strip, maintained at 4.2 K and current-biased close to the critical current. It exhibits an experimentally measured quantum efficiency of ~20% for 0.81 μm wavelength photons and negligible dark counts. © *2001 American Institute of Physics.*
[DOI: 10.1063/1.1388868]

Superconducting devices are the natural choice for fast and ultrasensitive optical detection, because of their quantum nature and low-noise, cryogenic operation environment. The superconducting energy gap 2Δ is two to three orders of magnitude lower than in a semiconductor, thus, photon absorption in a superconducting detector creates an avalanche electron charge two to three orders of magnitude higher for the same photon energy. This results in an enhanced resolution in energy-resolving devices, such as superconducting tunnel junctions,[1] and extends the range of detectable energies well into the infrared for photodetectors.[2] In addition, as we have recently demonstrated, energy relaxation time constants of excited electrons in superconductors are in the picosecond range for both the low-temperature[3] and high-temperature[4] superconductors, assuring the gigahertz repetition rate for superconducting photon counters.

The dynamics of the hotspot formation in a superconductor at temperature T below its critical temperature T_C, at the position where the photon is absorbed has been described before[5] and the supercurrent-assisted mechanism experimentally demonstrated in this work was theoretically studied in Ref. 6. Therefore, we only mention that the absorption of a photon with energy $\hbar\omega \gg 2\Delta$ creates, through electron–electron and electron–Debye–phonon interactions, a local nonequilibrium perturbation with a large number of excited hot electrons (above 300 in the case of NbN, excited with 790 nm wavelength light),[2] and an increase of the average electron temperature above T_C. This initial thermalization phase for ultrathin NbN films is characterized by the thermalization time $\tau_T = 6.5$ ps (Ref. 3) and results in the formation of a hotspot—a local nonsuperconducting region of the thermalization length $2\lambda_T$ [Fig. 1(a)]. After the initial thermalization, the resistive hotspot size grows [Fig. 1(b)] as hot electrons diffuse out of its center. At the same time, the supercurrent is expelled from the hotspot volume and is concentrated in the ''sidewalks'' between the hotspot and the edges of the film [Fig. 1(c)]. If the bias current I_{bias} is sufficient to exceed the critical current in the sidewalks, the phase slip centers are sprung[7] and a nonsuperconducting barrier is formed across the entire width w of the device [Fig. 1(d)], giving rise to a voltage signal, due to a collaborative effect of the bias current and the radiation quantum. For a given experiment, the response magnitude is proportional to the barrier resistance, however, in general, the current-assisted hotspot process creates a nonlinear, multidimensional space of operating parameters, such as w, I_{bias}, $\hbar\omega$, and T.

The hotspot formation process competes, of course, with the cooling process, as electrons diffusing out of the hotspot lose their energy through electron–phonon scattering. Thus, after the time depending on both the diffusion rate and the quasiparticle relaxation dynamics,[6] the hotspot heals itself, leading to the restoration of the superconducting path along the microbridge. As a result of the hotspot creation and relaxation processes, the NbN device switches temporarily be-

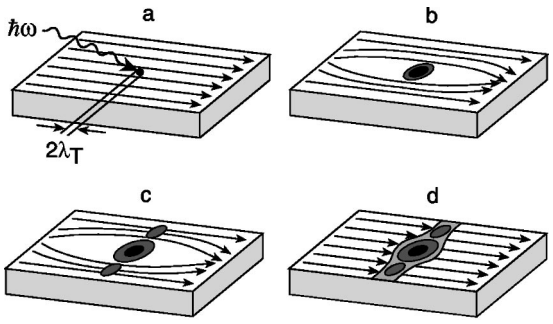

FIG. 1. Schematics of the supercurrent-assisted hotspot formation mechanism in an ultrathin and narrow superconducting strip, kept at temperature far below T_C are shown. The arrows indicate direction of the supercurrent flow.

[a]Also at: Department of Electrical and Computer Engineering and Laboratory for Laser Energetics, University of Rochester, Rochester, New York 14627-0231.

[b]Author to whom correspondence should be addressed: also at the Institute of Physics, Polish Academy of Sciences, PL-02904 Warszawa, Poland; electronic mail: sobolewski@ece.rochester.edu

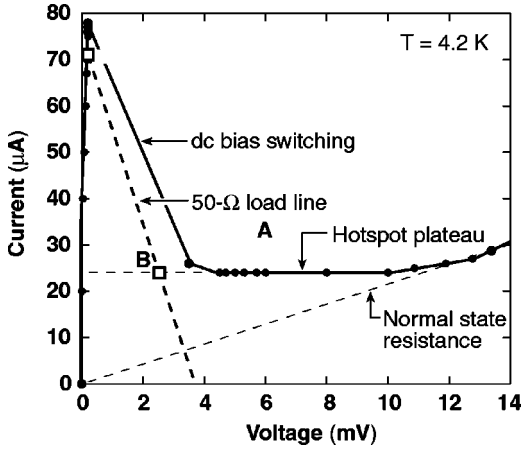

FIG. 2. $I-V$ characteristics of a 0.2 μm wide and 1.2 μm long NbN superconducting microbridge are shown. Point A denotes the initial detector bias level in the superconducting state and point B corresponds to the switched state upon absorbing a photon, leading a voltage pulse generation, before relaxing back to point A.

tween the superconducting and resistive states on a time scale of ~30 ps.

We have developed simple to manufacture, easy to operate, superconducting single photon detectors (SPDs) using nominally 0.2 μm wide and 1 μm long microbridges patterned from ultrathin (5 nm thick) NbN films deposited on sapphire substrate.[8] The microbridge was connected to the external circuit, via much thicker and larger, Au-coated contact pads. Figure 2 presents a current–voltage ($I-V$) characteristics of a NbN microbridge, operated at 4.2 K and biased using a voltage source. The characteristics are typical for a long superconducting constriction[9] and show that the bridge can be operated in either of the two distinct states: the superconducting (flux–flow) state *or* the resistive (hotspot) state. The hotspot plateau under dc conditions corresponds to the growing normal-state region, as the voltage across the device is increased, eventually reaching the bridge normal-state resistance, which in our case is approximately 500 Ω. The thick, dashed line represents a 50 Ω load line, when the device is connected to the output microwave transmission line. From Fig. 2, we see that the device I_C is approximately 78 μA.

For our experiments, a NbN SPD was mounted on a cold plate ($T=4.2$ K) inside an optical liquid-helium cryostat. We used two cold glass filters (inner glass window was at ~4.2 K) to block thermal radiation longer than 2.5 μm from the sample. The sample was dc biased through a bias tee and mounted on a rigid, 50 Ω coplanar transmission line with the ac output connected through a stainless-steel, semirigid coaxial cable to a cryogenic low-noise amplifier (placed inside the dewar), characterized by 30 dB gain and 1 to 2 GHz bandwidth. The noise temperature of our cryogenic amplifier was below 15 K, which yielded voltage fluctuations below 7 μV—several orders of magnitude below our signal levels. Outside the dewar, the signal passed through an isolator and a second broadband power amplifier (9 GHz; 20 dB gain) before going to a 6 GHz bandwidth single-shot oscilloscope for display, or to a 200 MHz voltage-level threshold counter for real-time event counting and statistical analysis. We worked with 100 fs wide, ~50 μm diameter optical pulses with a 1 kHz repetition rate at 0.4, 0.81, 1.55, and 2.1 μm wavelengths, with the bulk of the measurements performed using 0.81 μm photons. During our experiments, the fluence per pulse reaching the device plane inside the dewar was approximately $J_{\text{in}} \cong 1$ fJ/μm^2, and could be further attenuated using banks of neutral density filters, giving the total attenuation of 10^{-7}.

The actual fluence per pulse absorbed by our SPD, J_{abs}, can be estimated according to the relation $J_{\text{abs}}=J_{\text{in}}S_d\eta$, where S_d is the active area of the device and η is the radiation absorption coefficient of a metallic film, given by[10]

$$\eta = 4(R_s/Z_0)/[(R_s/Z_0)(n_{\text{sub}}+1)+1]^2, \tag{1}$$

where n_{sub} is the index of refraction of the SPD substrate, R_s is the surface resistance of the NbN film measured just above T_C, and $Z_0=377\,\Omega$ is the free-space impedance. For our sapphire substrate ($n_{\text{sub}}=1.72$), $\eta_{\max}=37\%$. η is frequency independent as long as n_{sub} remains frequency independent and the film is much smaller than the radiation skin depth, and can be regarded as the intrinsic quantum efficiency (QE) of our device.

For a device biased near, but below I_C (point A in Fig. 2), photon absorption instigated the supercurrent-assisted hotspot formation leading to a temporary switch from the superconducting state to the hotspot resistive state (point B in Fig. 2) along the 50 Ω load line. As a result, an output voltage was generated with a magnitude corresponding to the voltage level at point B, and that was independent of the actual photon energy, as long as the photon energy was sufficient to form a hotspot large enough to trigger the supercurrent redistribution effect. The response time of the voltage pulses followed the formation and subsequent healing of the resistive state induced by the photon absorption.[6]

The measured response of our SPDs (not shown) was indeed ''quantum'' or ''granular,'' in a sense that the voltage pulse amplitude was roughly the same (>400 mV after amplification, with a signal-to-noise ratio above 100:1) for all tested laser wavelengths. The response pulse width was ~100 ps, limited by the bandwidth of our chain of output amplifiers, and with negligible shot-to-shot jitter.

True single-photon counting requires that the photon detection probability has a linear dependence on the number of photons incident on the device. For a mean number of m photons per pulse, the probability $P(n)$ of absorbing n photons from a given pulse is $P(n)\sim(e^{-m}m^n)/(n!)$. When $m \ll 1$ (achieved by drastically attenuating the flux of photons incident on the SPD), the probability $P(n)$ simplifies to

$$P(n) \sim \frac{m^n}{n!}. \tag{2}$$

Consequently, the probability of absorbing one photon is proportional to m, the probability of detecting two photons is proportional to m^2, and so on.

Figure 3 shows the probability of the detector producing an output voltage pulse as a function of the average number $[J_{\text{in}}S_d/\hbar\omega]$ of 0.81 μm wavelength photons in a 100 fs pulse, incident on the device area, for two different values of I_{bias}. Since all photons arrive within the 100-fs-laser-pulse window, only spatial correlations (number of photons per device area) are important in the experiment. The left vertical

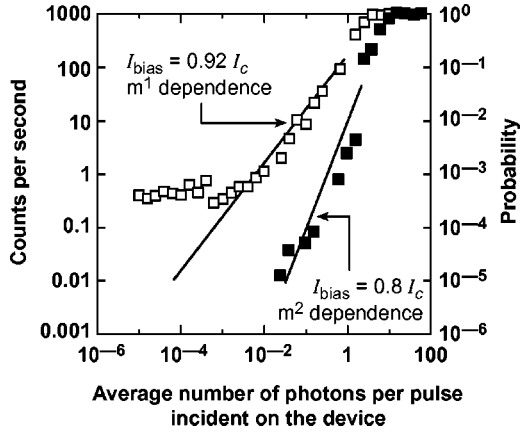

FIG. 3. Number of counts per second recorded by the NbN SPD versus the average number of photons per pulse incident upon the device, for two different bias current levels is shown. The solid lines correspond to the Eq. (4) theoretical predictions. The incident photon wavelength was 0.81 μm.

axis in Fig. 3 shows the experimental data i.e., the number of detector counts per second (equivalently, per 1000 laser pulses), based on the average number of counts detected by the SPD over a 10 s counting period for the highest photon doses, and up to 1000 s for the lowest. The counter threshold was adjusted to minimize spurious counts. The right vertical axis corresponds to the probability P of detecting an optical pulse. Open squares correspond to the SPD performance when it was biased at $0.92\,I_c$. For high incident photon fluxes, the detector managed to count all 1000 laser pulses in each second ($P=1$), without actually resolving the number of photons. For smaller fluxes, however, our experimental data show that for over four orders of magnitude, the detection probability decreases linearly with the decrease of the average number of incident photons, unambiguously demonstrating the single-photon detection mechanism. Since our experiment was performed in an optically unshielded environment (the detector was inside the dewar, but not in a dark box and only the main laboratory lights were off), at very low photon doses our experimental data points leveled off at 0.4 s^{-1} counts ($P=4\times10^{-4}$), which must be regarded as the laboratory single-photon background noise, where the background is essentially stray photons uncorrelated to the laser pulses. The intrinsic dark count rate of our SPD was below 0.001 s^{-1} ($P<10^{-6}$), which corresponded to zero number of detector responses over the time of 1000 s when its input was completely blocked.

From Fig. 3, we can estimate that the QE of our NbN microbridge is 20%, as the value corresponding to the probability of detecting a pulse containing an average of one photon incident upon the device. The practical detection efficiency of our SPD is, of course, much lower because of the very low S_d, as compared to the optical spot size. The maximization of detection efficiency is, however, strictly an engineering issue. Using proper coupling optics, the incident photon beam could be focused to a diffraction-limited spot size. At the same time, various geometrical configurations of the detector can be implemented, including a large-active-area meander-type design.

The 0.92-I_c detector bias was selected to achieve the single-photon detection with negligible dark counts (larger values of I_{bias}, resulted in dark counts associated with voltage oscillations in the metastable region). Lowering I_{bias}, on the other hand, led to the two-photon detection. Solid squares in Fig. 3 correspond to the same device, operated under the same conditions as discussed, but with $I_{\text{bias}}=0.8\,I_c$. We note immediately that our experimental data points now follow a quadratic dependence of detection probability showing the two-photon operation. The two-photon absorption, apparently, must form a larger hotspot size, needed to compensate for the smaller I_{bias}, but in this case, QE is significantly lower and is ~1%. At the same time, we do not see the laboratory photon background since the joint probability of two stray photons hitting the device area within the required space and time is negligibly small. Further reduction of I_{bias} (not shown in Fig. 3) resulted, unsurprisingly, in a cubic (three-photon detection) dependence of detection probability to the number of photons per pulse.

In conclusion, we have demonstrated that a supercurrent-assisted, hot-spot-formation mechanism can be implemented using an ultrathin NbN strip for ultrafast single-photon detection and counting of visible and infrared photons with an experimentally measured 20% QE for 0.81 μm photons and negligible dark counts. The bandwidth-limited measured response time was ~100 ps, corresponding to a 10 GHz photon counting rate. Already identified applications for our superconducting SPDs range from sensing ultraweak electroluminescence from submicron complementary metal–oxide–semiconductor very large scale integrated circuits,[11] to quantum communication systems.

The authors thank Aleksandr Verevkin, Kenneth Wilsher, Steven Kasapi, and Gerald Gilbert for helpful discussions and comments. This work was supported by Schlumberger SS, U.S. Office of Naval Research under Grant No. N00014-00-1-0237, and the NATO Linkage Grant No. CR-G.LG974662, and the Award No. RE-2227 of the U.S. Civilian Research and Development Foundation for the Independent States of the Former Soviet Union.

[1] A. Peacock, P. Verhoeve, N. Rando, A. van Dordrecht, B. G. Taylor, C. Erd, M. A. C. Perryman, R. Venn, J. Howlett, D. J. Goldie, J. Lumley, and M. Wallis, Nature (London) **381**, 135 (1996); R. J. Schoelkopf, S. H. Moseley, C. M. Stahle, P. Wahlgren, and P. Delsing, IEEE Trans. Appl. Supercond. **9**, 2935 (1999).
[2] K. S. Il'in, I. I. Milostnaya, A. A. Verevkin, G. N. Gol'tsman, E. M. Gershenzon, and R. Sobolewski, Appl. Phys. Lett. **73**, 3938 (1998).
[3] K. S. Il'in, M. Lindgren, M. Currie, A. D. Semenov, G. N. Gol'tsman, R. Sobolewski, S. I. Cherednichenko, and E. M. Gershenzon, Appl. Phys. Lett. **76**, 2752 (2000).
[4] M. Lindgren, M. Currie, C. Williams, T. Y. Hsiang, P. M. Fauchet, R. Sobolewski, S. H. Moffat, R. A. Hughes, J. S. Preston, and F. A. Hegmann, Appl. Phys. Lett. **74**, 853 (1999).
[5] A. M. Kadin and M. W. Johnson, Appl. Phys. Lett. **69**, 3938 (1996).
[6] A. D. Semenov, G. N. Gol'tsman, and A. Korneev, Physica C **351**, 349 (2001).
[7] M. Stuivinga, C. L. G. Ham, T. M. Klapwijk, and J. E. Mooij, J. Low Temp. Phys. **53**, 633 (1983).
[8] S. I. Cherednichenko, P. Yagoubov, K. S. Il'in, G. N. Gol'tsman, and E. M. Gershenzon, in *Proceedings of the Eighth International Symposium on Space Terahertz Technology* (Harvard University, Cambridge, MA, 1997), pp. 245–252.
[9] W. J. Skocpol, M. R. Beasley, and M. Tinkham, J. Appl. Phys. **45**, 4054 (1974).
[10] M. Born and E. Wolf, *Principles of Optics: Electromagnetic Theory of Propagation, Interference, and Diffraction of Light* 7th edition (Cambridge University Press, Cambridge, UK, 1999), pp. 752–758.
[11] J. C. Tsang and J. A. Kash, Appl. Phys. Lett. **70**, 889 (1997).